The 2016 super-Eddington outburst of SMC X-3: X-ray and optical properties and system parameters

L. J. Townsend,[1]⋆ J. A. Kennea,[2] M. J. Coe,[3] V. A. McBride,[1,4] D. A. H. Buckley[4]
P. A. Evans,[5] A. Udalski[6]

[1] *Department of Astronomy, University of Cape Town, Private Bag X3, Rondebosch, 7701, South Africa*
[2] *Department of Astronomy and Astrophysics, Pennsylvania State University, 525 Davey Lab, University Park, PA 16802, USA*
[3] *Physics and Astronomy, University of Southampton, Southampton SO17 1BJ, UK*
[4] *South African Astronomical Observatory, PO Box 9, Observatory 7935, South Africa*
[5] *Department of Physics and Astronomy, University of Leicester, Leicester LE1 7RH, UK*
[6] *Warsaw University Observatory, Aleje Ujazdowskie 4, PL-00-478 Warsaw, Poland*

ABSTRACT
On 2016 July 30 (MJD 57599), observations of the Small Magellanic Cloud by *Swift*/XRT found an increase in X-ray counts coming from a position consistent with the Be/X-ray binary pulsar SMC X-3. Follow-up observations on 2016 August 3 (MJD 57603) and 2016 August 10 (MJD 57610) revealed a rapidly increasing count rate and confirmed the onset of a new X-ray outburst from the system. Further monitoring by *Swift* began to uncover the enormity of the outburst, which peaked at 1.16×10^{39} erg/s on 2016 August 25 (MJD 57625). The system then began a gradual decline in flux which was still continuing at the time of writing, over 5 months after the initial detection. We explore the X-ray and optical behaviour of SMC X-3 between 2016 July 30 and 2016 December 18 during this extremely super-Eddington outburst. We apply a binary model to the spin-period evolution that takes into account the complex accretion changes over the outburst, to solve for the orbital parameters. Our results show SMC X-3 to be a system with a moderately low eccentricity amongst the Be/X-ray binary systems and have a dynamically determined orbital period statistically consistent with the prominent period measured in the OGLE optical light curve. The model fitting reveals complex changes in the neutron star spin that we attribute to a time variable or inhomogeneous disc. We conclude by showing that the measured increase in I-band flux from the counterpart during the outburst is reflected in the measured equivalent width of the H_α line emission, though the H_α emission itself seems variable on sub-day time-scales, not typical in these systems. We suggest that this may be a result of the neutron star interacting with an inhomogeneous disc.

Key words: X-rays: binaries - stars: emission line, Be - ephemerides - Magellanic Clouds

1 INTRODUCTION

High-mass X-ray binaries (HMXBs) are comprised of a compact object in orbit around an early-type star. Continuous or transient interactions between the two bodies cause X-rays to be produced on a range of time-scales and across a large range in luminosity. They have been observed in large numbers in the Milky Way and Magellanic Clouds, thanks to continuous monitoring from all-sky X-ray detectors and more focused surveys from several X-ray telescopes. HMXBs can be divided into 3 main groups: supergiant X-ray binaries (SGXRBs), Be-X/ray binaries (BeXRBs) and supergiant fast X-ray transients (SFXTs). SGXRBs are comprised of an early-type supergiant star and a neutron star or black hole and are mainly found in the Milky Way, though a few examples exist in the Small and Large Magellanic clouds (SMC, LMC). They can show persistent, sub-Eddington X-ray emission originating from direct accretion of the stellar wind onto the compact object, as well as more luminous emission through accretion via a stable disc around the compact object. BeXRBs are comprised of an early-type main-sequence or giant star that shows, or has shown, emission in the Balmer series. All but one system is known to host a neutron star; the other being a black hole (Casares et al. 2014).

They are found in large numbers in the Milky Way, SMC and LMC, and are the most numerous group of HMXBs known. They show significant variability in both time and luminosity, due to the wide range of observed binary parameters and the intrinsic variability of the Be star. In some circumstances, these systems can produce X-ray emission in excess of the Eddington limit for a nominal mass neutron star. SFXTs are recurring transient X-ray binaries, characterised by very short outbursts with fast rise times (e.g. Negueruela et al. 2006; Sguera et al. 2006). They are associated with OB supergiant stars, making them fundamentally different to both SGXRBs and BeXRBs, though there is some evidence to suggest that they may be evolutionarily linked to BeXRBs (Liu et al. 2011).

The SMC is an exceptional host galaxy when it comes to HMXBs; and specifically BeXRBs. We now know of 121 high-confidence HMXB systems in the SMC (Haberl & Sturm 2016). This is higher than the known population of HMXBs in the Milky Way, despite the significantly lower mass of the SMC. The most probable reason for this is recent (~ 400 Myr ago) bursts of star formation resulting in large numbers of massive, young stars. Work in this area is well documented (e.g. Dray 2006; Antoniou et al. 2010), though the details are beyond the scope of this paper. Of these 121 systems, 64 are confirmed pulsars (Haberl & Sturm 2016; Vasilopoulos et al. 2016). A detailed account of the optical and infra-red properties of this group of pulsating systems can be found in Coe & Kirk (2015).

The focus of this paper is the SMC BeXRB pulsar SMC X-3. As suggested by the name, SMC X-3 was the third X-ray source to be discovered in the SMC, by the SAS 3 satellite in 1977 (Li et al. 1977; Clark et al. 1978). In 2002, the *Rossi X-ray Timing Explorer (RXTE)* discovered a new pulsating X-ray source in the SMC, with a period of roughly 7.8 s (Corbet et al. 2003). Those authors detected this period several times during the following year, leading to the identification of a probable orbital period of ~45 d. It was not until 2004 that the association between this X-ray pulsar and SMC X-3 was made. Edge et al. (2004) used an archival *Chandra* observation to precisely locate SMC X-3 and determine a 7.78 s period in the light curve. The observation was made three days before a *RXTE* detection of the 7.8 s period, confirming the association of the *RXTE* and *Chandra* sources. The precise *Chandra* position from this work (00h52m05.7s, -72d26m05s (J2000.0), uncertainty 0.6 arcsec) was consistent with the position of the originally proposed optical counterpart to SMC X-3 (van Paradijs et al. 1977; Crampton et al. 1978). An optical modulation in long-term MACHO photometry was found at 44.86 d by Cowley & Schmidtke (2004). The authors note that this is very close to the X-ray period determined by Corbet et al. (2003) and conclude that it represents the binary period of the system. Edge (2005) also found a significant modulation in long-term OGLE photometry at 44.8 d, during a phase of apparent X-ray quiescence. The long-term *RXTE* light curve of SMC X-3 is presented in Galache et al. (2008). The authors determine a full X-ray ephemeris of MJD 52,250.9 ± 1.4 + 44.92n ± 0.06 d, where 44.92 d is the prominent modulation in the light curve and agrees well with the optically derived periods. In addition, the light curve seems to show distinct periods of X-ray activity lasting between ~ 200–400 d and separated by ~ 1000 d. Intriguingly, the authors note
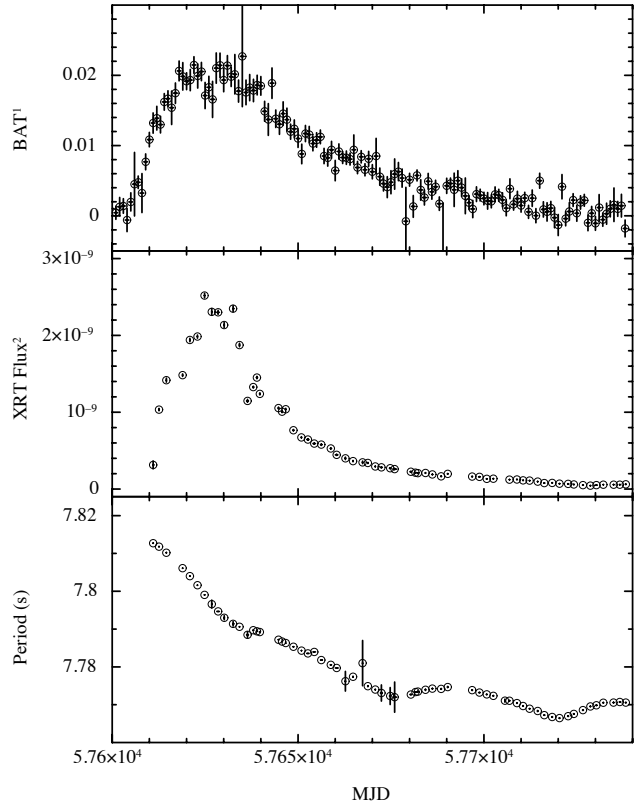

Figure 1. *Top panel*: *Swift*/BAT light curve of the 2016 outburst of SMC X-3. The BAT count rate is in units of counts/s/detector as reported by the BAT Transient Monitor (Krimm et al. 2013). *Middle panel*:*Swift*/XRT light curve of the 2016 outburst of SMC X-3. The XRT flux is in units of erg/s/cm^2 in the 0.5–10 keV range and has been calculated from spectral fitting of each observation. *Bottom panel*: Measured pulsar period of SMC X-3 during the outburst. The error bars are 1σ in all panels.

that there appears to be evidence of weak X-ray emission at apastron in the folded light curve and that the overall trend in the light curve is for a spin-down of the pulsar, despite the spin-up observed during X-ray active phases. Schmidtke et al. (2013) refine the optical period to 44.94±0.02 d using more recent OGLE III data. The authors also observe a dip in the folded light curve immediately before optical maximum, when the system is in an optically bright state. Finally, the spectral type of the counterpart was determined to be B1–1.5 IV–V (McBride et al. 2008).

In the following sections, we describe the recent super-Eddington outburst of SMC X-3. The original detection of the outburst was made by *MAXI* on 2016 August 08 (Negoro et al. 2016), although they were unable to identify conclusively that it was SMC X-3. The association was confirmed from multiple detections of the outburst by *Swift* (Kennea et al. 2016). The outburst was estimated to begin sometime between 2016 July 16 and 2016 July 30 based on *Swift/XRT* observations of the SMC, and was still ongoing over 5 months after this initial detection. In section 2, we present the *Swift* X-ray observations of the outburst between 2016 July 30 and 2016 December 18 and historical *RXTE* measurements of the long-term spin period. In section 3, we present the opti-
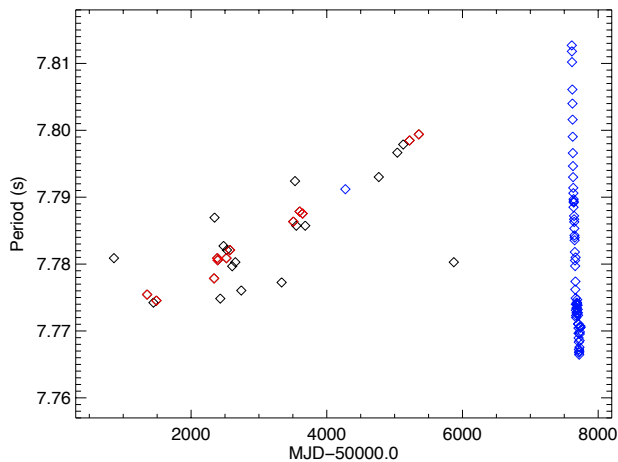
Figure 2. X-ray derived pulsed period history of SMC X-3. Black and red symbols denote *RXTE* period detections above the 99% and 99.99% confidence levels respectively. Blue symbols denote *Swift* detections of the pulse period during the current outburst and a single *XMM-Newton* detection at MJD 54274 found in the literature.

cal photometric and spectroscopic observations. The model used to determine the binary solution and mass accretion rate is discussed in section 4 and in section 5 we discuss the significance of this outburst and draw together our conclusions based on the combined optical and X-ray activity.

2 X-RAY OBSERVATIONS

In this section, we present the *Swift* BAT and XRT light curves and XRT timing of the 2016 super-Eddington outburst of SMC X-3. The *Swift* timing information is compared to the *RXTE* long-term spin period history.

2.1 Swift

The *Swift*/XRT has been observing the X-ray outburst of SMC X-3 since 2016 July 30 and continues to detect emission over 5 months later. We present data up to 2016 December 18. Fig. 1 shows the combined BAT and XRT light curves and the spin-period evolution of the neutron star during the outburst. The BAT light curve shown in the top panel is as reported by the BAT Transient Monitor (Krimm et al. 2013). The XRT data shown in the middle panel was extracted from a region of radius 20 pixels around the optical position of SMC X-3. The background was taken from an annulus between 90 and 110 pixels away from the central region. Due to the brightness of the source, the background contribution was small and was only used in the spectral analysis. Due to issues with calibration at low energies, we utilized data taken between 0.5–10 keV for spectral fitting. The XRT spectra are well fit by a simple absorbed power-law model. The power law index and absorption are typical for X-ray binaries in the SMC and do not show anything abnormal during this giant outburst. Using the flux from the spectral fits, we estimate the outburst reached a peak luminosity of 1.16×10^{39} erg/s,

assuming a source distance of 62 kpc[1] (Scowcroft et al. 2016 and references therein). This is above the Eddington limit for a $1.4\,\mathrm{M}_\odot$ neutron star by a factor of roughly 6. As can be seen in Fig. 1, SMC X-3 underwent a rapid increase in flux, before plateauing briefly at peak luminosity. It then entered a phase of more gradual decline. The luminosities calculated here are also using in the orbital model fitting described in section 4.

For the timing analysis, we used event data which was barycentrically corrected using the standard barycorr command. All the analysis was done using HEASOFT v6.19, and the latest XRT CALDB release (20160609). Each observation made with the XRT in Window Timing mode was run through a timing analysis pipeline to search for the spin period of the neutron star, which is presented in the final panel of Fig. 1. The period was determined using a standard Rayleighs Z_2^2 search (Buccheri et al. 1983), searching a period space around the known 7.78 s period of the source at a resolution of 10^{-6} s. Error estimation was performed using the Monte-Carlo method of Gotthelf et al. (1999). The folded pulse profile is fitted at the determined frequency and then used to generate 500 event files, utilizing Poissonian statistics, on which an identical period search is performed again. The error is then found by fitting a Gaussian model to the distribution of the periods found from these fake datasets.

2.2 RXTE

The position of SMC X-3 was observed by *RXTE* on a roughly weekly basis between 1999 and the end of the mission in 2012. As described in section 1, the eventual detection of a 7.78 s period by *RXTE* in 2002 led to the discovery that the known X-ray source, SMC X-3, was an accreting neutron star. In Fig. 2, we show the full spin period history of SMC X-3 as seen by *RXTE*. This figure is an extension of the spin period panel of Fig. 7 in Galache et al. (2008). In addition, we have included the period detections made by *Swift* during the current giant outburst and a single *XMM-Newton* period measurement found in the literature (Haberl et al. 2008).

Fig. 2 shows that the general spin-down trend observed in this system by Galache et al. (2008) has continued through the latter stages of the *RXTE* monitoring, right up to the start of the current giant outburst on MJD 57599. At this point we detect significant spin-up, unlike anything observed in this system before. The spin period measured at the time of writing is lower than the very first measurement by *RXTE*, showing that the momentum transferred by material accreted during the last 5 months has been greater than the momentum lost by magnetic breaking over the past 18 years. Klus et al. (2014) measure the long-term spin-down of SMC X-3 to be $0.00262 \pm 0.00003\,\mathrm{s\,yr^{-1}}$ and the average luminosity (during outburst) to be $(3.6 \pm 0.1) \times 10^{36}\,\mathrm{erg\,s^{-1}}$. This value is roughly 500 times lower than the spin-*up* value of $\sim -0.13\,\mathrm{s\,yr^{-1}}$ seen during the current outburst, showing

---

[1] Scowcroft et al. (2016) showed that the line-of-sight depth across the SMC varies around the average from -10 kpc in the East, to +10 kpc in the West. SMC X-3 lies roughly in the centre of this distribution and is therefore less likely to be at a significantly different distance than the average value.
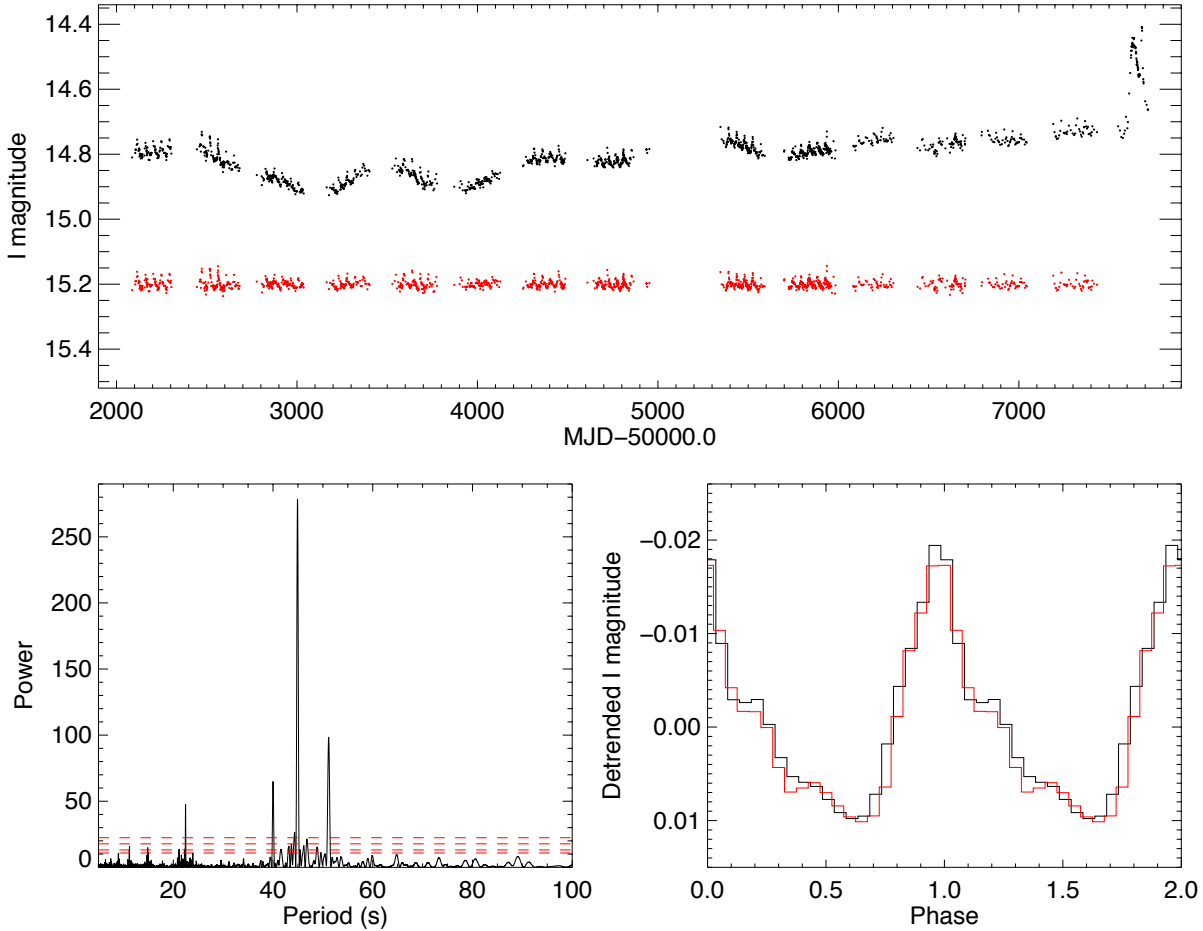
Figure 3. *Top panel*: OGLE III & IV light curve of SMC X-3 in the I-band (black). The detrended light curve is shown for comparison (red). For clarity, 15.2 magnitudes have been added to the detrended light curve. *Bottom-left panel*: Periodogram of the detrended OGLE light curve, excluding the recent outburst. The most prominent peak corresponds to a period of 44.918 d. The next highest peaks at periods of 40.00 d and 51.16 d are attributed to aliasing. There are smaller peaks visible, corresponding to harmonics of the main period. The dashed red lines are the 90, 99, 99.99 and 99.9999% confidence levels. *Bottom-right panel*: The detrended OGLE light curve folded at the 44.918 d period. OGLE III is in black and OGLE IV in red.

the significantly larger torques present during this outburst. Even during previous Type I outbursts recorded by *RXTE*, the spin period seems to continue increasing under low levels of accretion. This is probably evidence of extremely efficient accretion from a transient accretion disc in the current giant outburst.

3 OPTICAL OBSERVATIONS

In this section, we present optical photometry from the Optical Gravitational Lensing Experiment (OGLE) and optical spectroscopy from the Southern African Large Telescope (SALT) and South African Astronomical Observatory (SAAO) 1.9 m telescopes in South Africa, and the European Southern Observatory (ESO) 3.6 m telescope in Chile. We use the data to provide the most precise optical period measurement to date and show the evolution of the circumstellar disc over a long baseline, linking this to the X-ray activity in this system.

3.1 OGLE photometry

SMC X-3 was observed during the third and fourth phases of the OGLE project (Udalski et al. 2008; Udalski et al. 2015), resulting in a light curve spanning more than 14 years. The cadence varied from a few days to roughly a week during this time. The full light curve is shown in the top panel of Fig. 3. The black curve shows the combined OGLE III & IV data, whilst the red curve shows this light curve detrended with a 101 d sliding window function to remove the longer-term aperiodic variability, likely caused by changes in the size of the Be star disc. We manually removed the large outburst at the end of the light curve before detrending. The periodic modulations that can be seen throughout both light curves as regular spikes are typically thought to represent the orbital period of the system, though it is becoming clearer that this may not be entirely accurate (see discussion section). A large 0.4 magnitude jump in flux near the end of the light curve coincides with the current giant X-ray outburst. It is likely that a sudden growth in the disc has caused this and

Table 1. Observation time, telescope and equivalent width of each spectrum used in our analysis.

Date	MJD	Telescope	H_α EW
11 Nov 2001	52224	SAAO 1.9m	-11.4 ± 0.5
06 Nov 2003	52949	SAAO 1.9m	-12.1 ± 0.7
27 Oct 2005	53670	SAAO 1.9m	-11.8 ± 1.0
10 Nov 2006	54049	SAAO 1.9m	-10.2 ± 0.4
17 Sept 2007	54360	ESO 3.6m	-11.7 ± 0.3
11 Dec 2011	55906	NTT	-12.4 ± 0.2
04 Sept 2016	57635	SAAO 1.9m	-13.5 ± 0.7
06 Sept 2016	57637	SAAO 1.9m	-12.7 ± 0.6
06 Sept 2016	57637	SALT	-11.5 ± 0.1
11 Sept 2016	57642	SALT	-11.0 ± 0.1
13 Nov 2016	57705	SALT	-13.4 ± 0.1
25 Nov 2016	57717	SAAO 1.9m	-15.5 ± 0.4

triggered extensive accretion onto the orbiting neutron star. The optical outburst began on or just after MJD 57601, approximately 2 days after the first X-ray detection by *Swift*, though it is difficult to determine the precise onset due to the cadence of the light curve as well as the aforementioned uncertainty in the onset of the X-ray outburst.

The lower-left panel of Fig. 3 shows the periodogram of the detrended light curve. Most of the power is seen at a period of 44.918 ± 0.009 d., which agrees well with the optical value determined by Schmidtke et al. (2013) and the X-ray value determined by Galache et al. (2008). The first harmonic of the fundamental period is easily seen at 22.46 d. Higher order harmonics are also detected down to the sixth harmonic around 6.40 d. This results in quite a complex orbital profile (lower-right panel of Fig. 3). The OGLE III and IV light curves were folded separately and plotted for comparison. One can see that there is very little difference between the two phases, indicating that the period is very stable over more than a decade of observations. The profiles are also highly skewed in a 'fast rise, exponential decay' shape. This shape is indicative of the modulation being related to the binary period of the system (e.g. Bird et al. 2012). The ephemeris of peak flux is MJD 57682.14 ± 0.37. This will be discussed further in section 5 in the context of the orbital ephemeris from binary model fitting.

3.2 Spectroscopy

Observations were obtained from the Southern African Large Telescope (SALT) and South African Astronomical Observatory (SAAO) 1.9 m telescope just after the peak of the X-ray outburst to measure the shape and equivalent width of the H_α emission line, and to see if any other features were present. These were compared with several archival spectra from the SAAO 1.9 m and ESO 3.6 m telescopes obtained sporadically over the past ~20 years. The details of these observations, and the measured equivalent widths, are shown in Table 1.

Fig. 4 shows the H_α equivalent width measurement from each of the archival spectra obtained with the SAAO 1.9 m telescope and the ESO 3.6 m and NTT telescopes, as well as the SAAO 1.9 m and SALT/RSS spectra taken during the current outburst. Despite large gaps in the coverage of SMC X-3, there is moderate evidence that the circumstellar disc
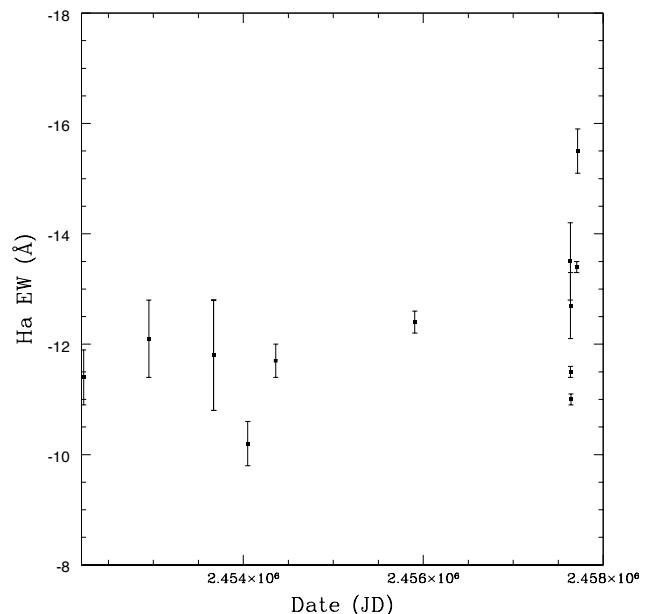
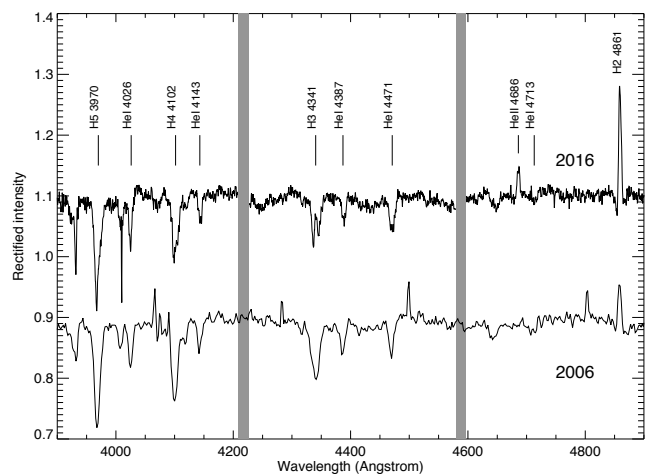**Figure 4.** Measured values of the H_α equivalent width from the spectra listed in Table 1.

Figure 5. ESO 3.6 m spectrum from 2006 and SALT RSS spectrum taken during the current X-ray outburst. The spectra are rectified and offset from 1.0 by 0.1 on either side for clarity. The vertical grey lines represent the chip gaps in the SALT CCD. The spiky feature near 4050 Å in the NTT spectrum is a CCD artefact.

around the Be star has grown in recent months; as suggested by the OGLE photometry. However, there is also evidence for rapid variability in the line emission that is unexpected in this type of binary system, even during a large outburst. This point is discussed in section 5.

In addition to these data, we obtained a blue SALT/RSS spectrum to look for the presence of helium in emission. We compare this spectrum to an ESO 3.6 m spectrum obtained in September 2006 (see McBride et al. 2008 for a description of the ESO observation and the data reduction). The blue SALT/RSS spectrum was obtained using the

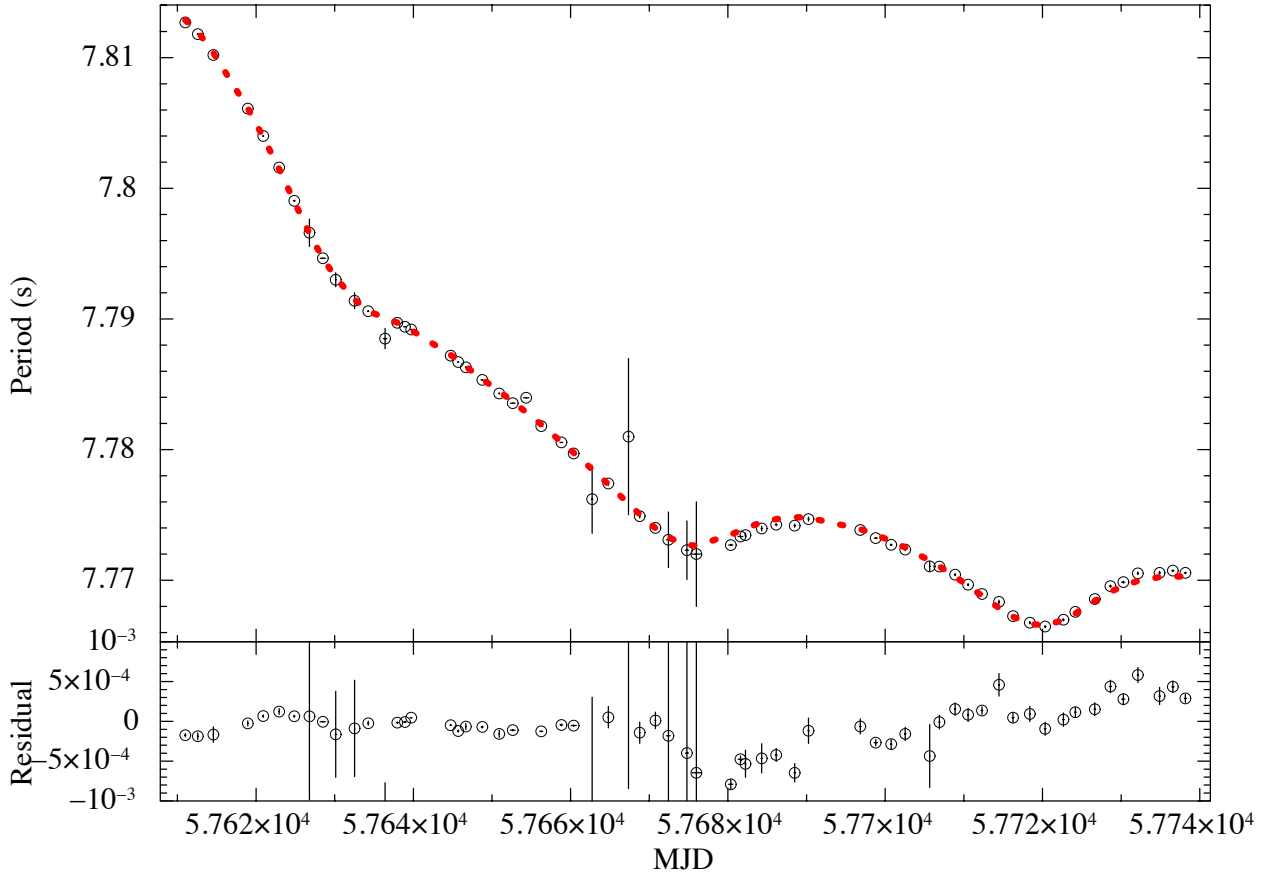**Figure 6.** *Top panel*: *Swift* period measurements as presented in Fig. 1, with the combined binary and spin-up model over-plotted in red. *Lower panel*: Residuals of the fit.

PG2300 grating at an angle of 30.5 degrees, yielding a resolution of 2.1 Å. Fig. 5 shows the archival ESO spectrum and the recent SALT spectrum taken during the outburst. He II 4686 is clearly in emission during the outburst and not present in quiescence[2]. This is likely evidence of a transient accretion disc around the neutron star. The H_β line shows evidence of a very narrow emission component superimposed on a rotationally broadened absorption line, typical of many early-type emission line stars. The emission component is also stronger than it was in 2006. Emission in H_γ and possibly H_δ is also apparent in the 2016 SALT spectrum. This is further good evidence that the disc has grown in the time between these observations.

4   ORBITAL SOLUTION

The measured pulsar period of SMC X-3 shows a significant amount of variability during the outburst, overall showing a decrease in period due to pulsar spin-up, but also showing modulation due to Doppler shift caused by orbital motion. We attempted to model the evolution of the pulsar period utilizing several models. Firstly we fit the data with a model

comprising of a simple spin-up (i.e. constant $\dot{P}$), with orbital modulation. Unfortunately we were not able to obtain an adequate fit to the data utilizing this model, suggesting that the spin-up of the pulsar was not linear.

In an attempt to model this, we followed the example of Takagi et al. (2016) which modelled $\dot{P}$ utilizing the equation of Ghosh & Lamb (1979), which suggests that the spin-up of a pulsar is proportional to $L_{37}^{6/7}$, where L_{37} is the bolometric luminosity of the pulsar in units of 10^{37} erg/s. We simplified this by assuming that all the values other than L_{37} and P in equation 3 of Takagi et al. (2016) can be combined into a constant. Note that for L_{37} we simply use a model fitted luminosity based on the spectral fitting described in section 2, and corrected for a standard SMC distance of 62 kpc. We assume that the correction from this luminosity to a bolometric luminosity is constant, and include that in the fitted constant parameter. Therefore the fitted model (hereafter referred to as GL79) becomes:

$$\dot{P} = C \times P^2 \times L_{37}(0.5 - 10 keV)^{6/7} \qquad (1)$$

Fitting this model, including an orbital Doppler shift, to our data provides a much improved fit over a simple linear $\dot{P}$, however the model underestimates the spin-up in the latter parts of the outburst. In order to compensate for this, we

---

[2] Quiescence is confirmed by the lack of pulsations detected with *RXTE* as shown in Fig. 2

Table 2. Binary solutions obtained in this work.

Parameter		GL79 model (fixed index)	GL79 model (free index)	GL79 model (data subset)	$\ddot{P}$ model (data subset)
Orbital period	$P_{orbital}$ (d)	45.4 ± 0.5	45.2 ± 0.5	44.7 ± 0.1	44.6 ± 0.2
Projected semimajor axis	$a_x \sin i$ (light-s)	198 ± 8	195 ± 7	192 ± 2	190 ± 5
Longitude of periastron	ω (^{o})	209 ± 8	204 ± 7	208 ± 2	202 ± 6
Eccentricity	e	0.20 ± 0.02	0.21 ± 0.02	0.24 ± 0.01	0.22 ± 0.02
Orbital epoch	$\tau_{periastron}$ (MJD)	57676.3 ± 1.1	57676.0 ± 1.1	57677.0 ± 0.2	57676.6 ± 0.7
GL79 index	GL79 index	6/7 (fixed)	0.73 ± 0.02	0.95 ± 0.02	N/A
First derivative of P	$\dot{P}$ (10^{-10}ss^{-1})	-4.9 ± 0.7	N/A	N/A	-14.9 ± 0.2
Second derivative of P	$\ddot{P}$ (10^{-16}ss^{-1})	N/A	N/A	N/A	4.50 ± 0.02
Goodness of fit	χ^2_ν (d.o.f.)	15412 (55)	14240 (55)	58 (32)	230 (31)

attempted three variations of the model. Firstly we added in an additional $\dot{P}$ value to account for the poor fit in the latter parts of the outburst. Secondly we allowed the luminosity index in equation 1 to be a fitted parameter. Thirdly we fit the variable index model to a subset of the data cut at the point where the luminosity is estimated to have dropped below the Eddington limit, in the assumption that this would remove some of the most complex spin-period changes near the beginning of the outburst. In the first two cases the fit was improved and converge on realistic binary parameters, though the resulting χ^2 values are poor. The fit to the data subset produced the best fit in terms of χ^2, but a more complex spin-period model is still clearly required. We stress that this model is simply a parametrisation of the data, and does not represent a realistic model explaining the spin period evolution. However, in fitting the underlying period evolution like this, it allows us to accurately determine the orbital parameters of the system. Our best fitting solution to the full dataset is presented in Fig. 6 and all model parameters are presented in Table 2. It is apparent that the model struggles to fit the data where there are sharp or complex changes in the spin period (e.g. near MJD 57675), which are likely due to some higher order spin variability caused by (for example) a time-variable or clumpy stellar wind that is impossible to model. Indeed, Ghosh & Lamb (1979) assume accretion is from an aligned disc, whereas in reality the accretion in a Be/X-ray binary is likely to be more complex than this, which may affect the relationship. The assumption that the correction from XRT flux to bolometric flux is a constant throughout the outburst is also likely not entirely accurate, given the evidence of spectral evolution throughout the outburst.

The reason for the poor χ^2 fits shown in Table 2 is that there are higher order variations in the spin-up of the neutron star that we are unable to model. This does not mean that the binary parameters cannot be determined, just that the model does not account for the more complex changes in spin-up caused by a variable accretion rate. In order to test whether our binary model does reliably determine the orbital parameters in this system, we applied a simple $\dot{P} + \ddot{P}$ model to the data that does not take into account the luminosity of the outburst. This removes the uncertainty arising from our assumption of a constant bolometric flux correction, but means that rapid changes in the spin period are less likely to be accounted for than in the previous model. Indeed, this proved to be the case as the model was unable to converge to a physically realistic set of parameters. We

applied the same model to the subset of the data described above. The result of this fit is included in Table 2 along with the other fits. One can see that the fits to the subset of data that excluded the initial super-Eddington part of the outburst are better than fits to the full dataset. This may be due to more complex spin period variability being present during the onset of the outburst, or because the errors on our spin period measurements are being underestimated at higher luminosities due to an imperfect model of the shape of the pulse profile. The similarity of the results from the two model fits to the data subset also confirm that we are reliably extracting the true binary parameters.

In fitting the $\ddot{P}$ model, we adjusted the errors on the timing data such that the χ^2_ν became unity. This was done to avoid underestimating the parameter errors in this fit. It assumes that our model is completely correct, which it is unlikely to be, due to the complex accretion changes evident in this outburst. The underlying binary parameters are unaffected by this and are relatively unchanged across the four models, despite the spin-up results being significantly different. Therefore, we are confident in our resulting parameters but chose to present the most conservative errors on these parameters given the uncertainty in the spin-up measurements.

5 DISCUSSION

At the time of writing, SMC X-3 was still being detected at a high level of confidence with *Swift* having been in X-ray outburst for 5 months. It is one of the longest and brightest outbursts ever recorded from a BeXRB. We discuss the results of our observations and compare SMC X-3 to the known population of BeXRBs.

5.1 System parameters and mass function

In trying to model the binary orbit of SMC X-3, we were using a dataset containing incredibly complex variations in the measured neutron star spin period. Thus, it was very difficult to properly account for the whole outburst without modifying certain accretion models or taking subsets of the data. We attribute the variations present beyond the standard accretion models to be from a time-variable or clumpy circumstellar disc from which the neutron star accretes. This seems to satisfy what is observed in the H$_\alpha$ equivalent width

measurements, which are indicative of rapid density or temperature variations in the disc. The reason for not fixing the binary period at the very precise value determined from the optical light curve, is because of the growing evidence that this optical period does not necessarily represent the exact binary period (e.g. Vasilopoulos et al. 2014, Bird et al. 2012). Whilst in this case we presume that the binary period is very close to the period in the optical data and the *RXTE* data presented in Galache et al. (2008), we cannot be certain enough to fix the parameter in the final fit. During the fitting process, we did fix the period to 44.918 s to observe the result, though in all of the three cases presented in Table 2 this resulted in poorer χ_ν^2 values without significantly changing the other binary parameters. The fitted orbital period is consistent with the optical period to within $1\,\sigma$ in the GL97 fits to the full dataset and within $2\,\sigma$ in the GL79 and $\ddot{P}$ model fits to the subset of data.

The binary parameters are known in 7 other BeXRB systems in the SMC (Townsend et al. 2011; Coe et al. 2015). When compared to this group, SMC X-3 seems to have a lower than expected eccentricity for its orbital period. It sits in between the 'normal' BeXRB systems and the group of low eccentricity systems suggested by Pfahl et al. (2002) in Fig. 6 of Townsend et al. (2011), lending support to the idea that these systems are not formed through channels with either a large or small natal supernova kick. Instead, it seems more likely that there is a broad range of eccentricities in BeXRBs, regardless of their orbital period. SMC X-3 also has the highest measured projected semi-major axis of the SMC systems to date, despite having a low eccentricity. The mass function derived from these parameters is $3.7\,\mathrm{M_\odot}$, typical of other BeXRBs.

5.2 Circumstellar disc

The stable and highly significant periodicity measured in the OGLE light curve is likely to be very close to the binary period of SMC X-3. This period is also seen in the long-term *RXTE* light curve (Galache et al. 2008), making this even more probable. If this is the case, then the difference in the measured ephemerides becomes intriguing. We find an ephemeris of maximum optical flux of MJD 57682.14 ± 0.37, whereas the dynamically determined orbital ephemeris is MJD 57676.6 ± 0.7 (for the median of the fits). This is unchanged within the error when the period is fixed to the optical value. This suggests that the peak in optical flux occurs roughly 6 days after periastron, and that this offset is stable over more than a decade. Smoothed-Particle Hydrodynamic simulations (Okazaki et al. 2002) show that for any non-zero eccentricity the neutron star distorts the disc shape as it goes through periastron. This distortion increases the surface area of the circumstellar disc leading to an optical flare or enhancement. A lag of ~ 6 days is an indication of how long this process takes, probably related to the disc viscosity. This effect if observed in other well-known systems, such as PSR B1259–63. The ephemeris derived from the *RXTE* light curve is not precise enough to extrapolate forward and compare to the other ephemerides.

The OGLE light curve and the historical H$_\alpha$ measurements suggest the disc in SMC X-3 has been very stable over more than a decade. Some of the Be stars in BeXRBs do exhibit this behaviour, though it is more common to see
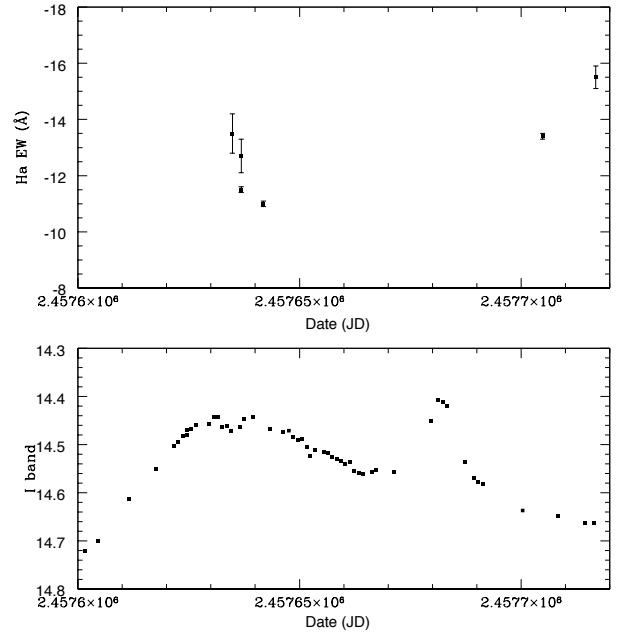

Figure 7. Measured H$_\alpha$ emission during the X-ray outburst of SMC X-3 plotting above the corresponding OGLE I-band photometry.

some large-scale variability on time-scales of a few years[3]. The increase in optical flux coincides with the X-ray outburst, meaning the circumstellar disc is the source of extra material for this outburst, though the brightening of 0.3 mag is still only a moderate rise given the enormity of the X-ray outburst. The consistently single peaked H$_\alpha$ emission seems to point towards a disc that is not highly inclined to our line-of-sight, meaning a large increase in the size of the disc is not being hidden from us by a projected inclination effect.

Spectroscopic coverage of SMC X-3 has been sparse, making it hard to say whether the disc emission in H$_\alpha$ mimics the long-term broadband optical emission. However, we have observed the H$_\alpha$ emission to be variable on shorter time-scales, not seen in the optical light curve. Fig. 7 shows the measured H$_\alpha$ emission during the outburst and the corresponding I-band flux during this time. One can see that the H$_\alpha$ emission changes by at least 1 Å in a matter of hours and by as much as 50 % in a few days. This variability is not reflected in the I-band flux. To check that the errors are not being underestimated, we measured the equivalent widths in several different ways: Gaussian fitting, randomised continuum fitting using a Monte-Carlo method and using the STARLINK/DIPSO software, where the errors are calculated using the prescriptions given by Howarth & Phillips (1986). In all cases, the error bars were similar and confirmed the variability must be intrinsic to the source. Unfortunately, the coverage around any given orbit of the neutron star is not sufficient to say if this is linked to orbital phase in some way. The cause could be the interaction of the neutron star with inhomogeneities in the expanded disc, but

---

[3] See the OGLE XROM data analysis system (Udalski 2008) for long-term light curves of most BeXRBs in the SMC.

this is also difficult to confirm without somehow linking this to the spin-period variations seen in section 4 and without explaining the lack of variability in the optical light curve.

6   CONCLUSIONS

This paper presents X-ray and optical observations made between 2016 July 30 and 2016 December 18 during the first 5 months of the giant X-ray outburst of SMC X-3. The peak X-ray luminosity is far in excess of the Eddington limit for a canonical mass neutron star, suggesting the presence of highly collimated or beamed emission. The complex period changes, likely caused by variable accretion torques, have been untangled from the orbital modulations allowing us to measure the binary parameters. We show the binary parameters of this system are typical of other BeXRB systems, though perhaps somewhat on the edge of the distribution of eccentricities of 'normal' BeXRB systems given the longer binary period. When compared to historical spin period measurements made by *RXTE*, the pulsar is seen to deviate from a state of constant spin-down to an extremely rapid spin-up that returned the neutron star spin period to that observed 18 years ago, in just 5 months.

We suggest the optical period of 44.918 days is the true binary period, being consistent with the long-term X-ray period and the dynamical period. However, the ephemeris shows the optical emission is delayed by around 6 days from periastron, which may be linked to viscous time-scales in the disc as it is being distorted by the neutron star. The H$_\alpha$ emission from the disc is variable on short time-scales which may be linked to the disc being inhomogeneous or time-variable and is probably associated with the complex spin-period changes that are observed, though the data are not sufficient to confirm this hypothesis. We also observe He II in emission, showing the reservoir of material is sufficient to fuel an accretion disc around the neutron star. This is often not seen in BeXRBs and reflects the enormity of this outburst.

REFERENCES

Antoniou V., Zezas A., Hatzidimitriou D., Kalogera V., 2010, ApJ, 716, L140
Bird A. J., Coe M. J., McBride V. A., Udalski A., 2012, MNRAS, 423, 3663
Buccheri R., et al., 1983, A&A, 128, 245
Casares J., Negueruela I., Ribó M., Ribas I., Paredes J. M., Herrero A., Simón-Díaz S., 2014, Nature, 505, 378
Clark G., Doxsey R., Li F., Jernigan J. G., van Paradijs J., 1978, ApJ, 221, L37
Coe M. J., Kirk J., 2015, MNRAS, 452, 969
Coe M. J., Bartlett E. S., Bird A. J., Haberl F., Kennea J. A., McBride V. A., Townsend L. J., Udalski A., 2015, MNRAS, 447, 2387
Corbet R. H. D., Edge W. R. T., Laycock S., Coe M. J., Markwardt C. B., Marshall F. E., 2003, in AAS/High Energy Astrophysics Division #7. p. 629
Cowley A. P., Schmidtke P. C., 2004, AJ, 128, 709
Crampton D., Hutchings J. B., Cowley A. P., 1978, ApJ, 223, L79
Dray L. M., 2006, MNRAS, 370, 2079
Edge W. R. T., 2005, PhD thesis, University of Southampton (United Kingdom), England
Edge W. R. T., Coe M. J., Corbet R. H. D., Markwardt C. B., Laycock S., 2004, The Astronomer's Telegram, 225
Galache J. L., Corbet R. H. D., Coe M. J., Laycock S., Schurch M. P. E., Markwardt C., Marshall F. E., Lochner J., 2008, ApJS, 177, 189
Ghosh P., Lamb F. K., 1979, ApJ, 234, 296
Gotthelf E. V., Vasisht G., Dotani T., 1999, ApJ, 522, L49
Haberl F., Sturm R., 2016, A&A, 586, A81
Haberl F., Eger P., Pietsch W., 2008, A&A, 489, 327
Howarth I. D., Phillips A. P., 1986, MNRAS, 222, 809
Kennea J. A., et al., 2016, The Astronomer's Telegram, 9362
Klus H., Ho W. C. G., Coe M. J., Corbet R. H. D., Townsend L. J., 2014, MNRAS, 437, 3863
Krimm H. A., et al., 2013, ApJS, 209, 14
Li F., Jernigan G., Clark G., 1977, IAU Circ., 3125
Liu Q. Z., Chaty S., Yan J. Z., 2011, MNRAS, 415, 3349
McBride V. A., Coe M. J., Negueruela I., Schurch M. P. E., McGowan K. E., 2008, MNRAS, 388, 1198
Negoro H., et al., 2016, The Astronomer's Telegram, 9348
Negueruela I., Smith D. M., Reig P., Chaty S., Torrejón J. M., 2006, in Wilson A., ed., ESA Special Publication Vol. 604, The X-ray Universe 2005. p. 165 (arXiv:astro-ph/0511088)
Okazaki A. T., Bate M. R., Ogilvie G. I., Pringle J. E., 2002, MNRAS, 337, 967
Pfahl E., Rappaport S., Podsiadlowski P., Spruit H., 2002, ApJ, 574, 364
Schmidtke P. C., Cowley A. P., Udalski A., 2013, MNRAS, 431, 252
Scowcroft V., Freedman W. L., Madore B. F., Monson A., Persson S. E., Rich J., Seibert M., Rigby J. R., 2016, ApJ, 816, 49
Sguera V., et al., 2006, ApJ, 646, 452
Takagi T., Mihara T., Sugizaki M., Makishima K., Morii M., 2016, PASJ, 68, S13
Townsend L. J., Coe M. J., Corbet R. H. D., Hill A. B., 2011, MNRAS, 416, 1556
Udalski A., 2008, Acta Astron., 58, 187
Udalski A., Szymanski M. K., Soszynski I., Poleski R., 2008, Acta Astron., 58, 69
Udalski A., Szymański M. K., Szymański G., 2015, Acta Astron., 65, 1
Vasilopoulos G., Haberl F., Sturm R., Maggi P., Udalski A., 2014, A&A, 567, A129
Vasilopoulos G., Haberl F., Antoniou V., Zezas A., 2016, The Astronomer's Telegram, 9229
van Paradijs J., Schlosser W., Tarenghi M., Sanduleak N., Philip A. G. D., 1977, IAU Circ., 3134

This paper has been typeset from a T$_{\rm E}$X/L$^{\rm A}$T$_{\rm E}$X file prepared by the author.